












Chasing the two-Higgs doublet model in the di-Higgs production


Syuhei Iguro,^{} Teppei Kitahara,^{} Yuji Omura,^{}
and Hantian Zhang^{}


 *Institute for Theoretical Particle Physics (TTP), Karlsruhe Institute of Technology (KIT),
Engesserstraße 7, 76131 Karlsruhe, Germany*


 *Institute for Astroparticle Physics (IAP), KIT, Hermann-von-Helmholtz-Platz 1,
76344 Eggenstein-Leopoldshafen, Germany*

 *Institute for Advanced Research, Nagoya University, Nagoya 464-8601, Japan*

 *Kobayashi-Maskawa Institute for the Origin of Particles and the Universe,
Nagoya University, Nagoya 464-8602, Japan*

 *KEK Theory Center, IPNS, KEK, Tsukuba 305-0801, Japan*

 *CAS Key Laboratory of Theoretical Physics, Institute of Theoretical Physics,
Chinese Academy of Sciences, Beijing 100190, China*

 *Department of Physics, Kindai University, Higashi-Osaka, Osaka 577-8502, Japan*

E-mail: igurosyuhei@gmail.com, teppeik@kmi.nagoya-u.ac.jp,
yomura@phys.kindai.ac.jp, hantian.zhang@kit.edu

Abstract

We investigate the di-Higgs productions at the Large Hadron Collider in the two-Higgs doublet model. In particular, we study the productions of an extra scalar, ϕ ($\phi = H, A$), in association with the Standard Model (SM)-like Higgs boson, h . We consider a scenario that the additional scalars have a large top-Yukawa interaction in the Higgs alignment limit. Then, the leading contribution to the production comes from the loop-induced gluon-fusion channel $gg \rightarrow h\phi$. Similar to the SM Higgs pair production, these $h\phi$ productions are sensitive to the Higgs potential as well as the Yukawa couplings. In this paper, we calculate these $h\phi$ production cross sections at the leading order, taking into account the theoretical constraints from the perturbative unitarity and vacuum stability bounds as well as the precision measurements from the Higgs and flavor physics. Furthermore, we scrutinize the di-Higgs production in the parameter spaces that can explain the excesses around 100 GeV in di- τ and di-photon and/or the muon $g - 2$ anomaly.

KEYWORDS: Multi-Higgs Models, Di-Higgs Production, Large Hadron Collider

1 Introduction

The spontaneous symmetry breaking of $SU(2)_L \times U(1)_Y$ is caused by a Higgs field in the Standard Model (SM) [1, 2], where the Higgs potential is given by a negative mass squared and a quartic coupling, and the Higgs obtains non-vanishing vacuum expectation value (VEV). Through couplings between the Higgs and the other SM fields, fermions obtain their masses and the $SU(2)_L$ gauge bosons acquire the masses by eating the Nambu–Goldstone (NG) boson [3–5]. This picture is very successful in explaining experimental results. The origin of the negative mass squared is, however, unknown, and hence motivates the further understanding of the Higgs sector. There may be many Higgs fields and the scalar potential may be more complicated than our expectation.

One good way to reveal our vacuum structure given by the scalar potential is to test signals involving (extra) scalars in the final state at the Large Hadron Collider (LHC). The Higgs boson pair production, for instance, gives information about the triple Higgs coupling [6, 7]. Precise calculations of the dominant contribution in the SM, $gg \rightarrow hh$, have been performed at next-to-leading order (NLO) QCD accuracy [8–18], where h is the SM (-like) Higgs boson (in the new physics models). Its frontier has been pushing up to next-to-next-to-next-to-leading order (N³LO) QCD [19–28] and NLO electroweak (EW) [29, 30] in various approximations. It has been still difficult to test the scalar potential parameters directly at the LHC due to the small Higgs-pair production cross section compared to the huge QCD background [31, 32]. Nevertheless, thanks to the accumulating luminosity at the LHC and improvements in the flavor tagging algorithm [33, 34], the measurement of the Higgs-pair production has provided the profound information of the triple Higgs coupling and thus the shape of the Higgs potential [35–46]. The future prospect is discussed in Refs. [7, 47].

Multi-Higgs doublet models often appear as low-energy effective theories: the supersymmetric SM [48, 49], left-right symmetric model [50], and so on. Therefore, it would be interesting to investigate and summarize the experimental constraints on the parameter space of new physics models with extra Higgs doublets. After the SM Higgs discovery in 2012 [51, 52], it has turned out that its interaction is well consistent with the SM prediction within the current experimental and theoretical uncertainties [53, 54]. The fact may imply that the additional scalars live in the considerably high energy, leading to the decoupling feature, or are hidden from the measurements by the *Higgs alignment* where the additional Higgs doublets do not mix with the SM-like Higgs doublet. In this paper, we pursue the second possibility, and propose a way to probe a relatively light neutral scalar through di-Higgs production channels.

We will consider the two-Higgs doublet model (2HDM) as a working example. There are many motivations for the light additional scalars with the large mass differences among them. Baryon asymmetry of the universe (BAU) is a one of the big mysteries of the modern particle physics [55]. It is known that the CP violation of the

SM, namely the complex phase of the CKM matrix, is not large enough to generate the observed BAU. In addition, the observed Higgs mass, *i.e.*, 125 GeV, is too heavy for the strong first-order phase transition (SFOPT). For a successful SFOPT, the modification of the Higgs potential is necessary and the extension of the Higgs sector is well motivated [56–59]. It is shown that an additional $\mathcal{O}(1)$ top-Yukawa coupling can provide the large CP violation [60]. The joint explanation of the radiative neutrino mass generation with a light scalar scenario is also discussed [61–63].

Moreover, a light (pseudo) scalar would explain the discrepancy in the muon anomalous magnetic moment (muon $g-2$) [64–67]. The recent evaluations of a window observable for the hadronic vacuum polarization based on lattice QCD simulation [68] are shown in Refs. [69–74], and a large discrepancy with the $e^+e^- \rightarrow 2\pi$ data has been reported in Refs. [75–77]. In the flavor-conserving 2HDM where only flavor-diagonal Yukawa interaction is introduced, the light scalar in the Barr-Zee two-loop diagram could explain the discrepancy in the muon $g-2$ anomaly [78]. A large mass gap between the lightest scalar and the charged scalar is necessary to avoid collider constraints.

In recent years, not significant enough but mild excesses have been reported around 95 GeV in $\tau\bar{\tau}$ [79] and $\gamma\gamma$ [80] resonance searches by the CMS collaboration, and in $b\bar{b}$ mode by the LEP experiment [81]. In Ref. [82], it is shown that an additional light scalar with a CP-odd pseudo-scalar interaction with $t\bar{t}$ can still provide a viable solution to the $\tau\bar{\tau}$ excess reported by the CMS, while the CP-even scalar explanation is shown to be difficult. Within this scenario, the production cross section of $pp \rightarrow t\bar{t} + \tau\bar{\tau}$ is suppressed because of the cancellation among diagrams. We will show that the measurement of the di-Higgs production via the triangle and box diagrams provides an powerful cross check for this pseudo-scalar solution.

In this paper, motivated by aforementioned issues, we investigate the impact of $h\phi$ production at the current and high luminosity (HL) LHC, where $\phi = H$ and A are CP-even and -odd additional neutral scalars, respectively. We show the production cross sections in a plane of relevant model parameters, and discuss the phenomenological impact especially motivated by those excesses. Calculations in the relevant beyond SM scenarios are addressed Refs. [83–92]. In particular, various Higgs-pair production cross sections in the gluon-fusion channel are calculated based on the benchmark model parameters [90].

The outline of the paper is given as follows. In Sec. 2, we introduce a two-Higgs doublet model and summarize relevant model parameters for our analysis. We investigate the $h\phi$ production in Sec. 3. Furthermore, the phenomenological impact of the $h\phi$ production is given along with relevant constraints from flavor physics and Higgs precision measurements. Section 4 is devoted to the conclusion.

2 Two Higgs doublet model (2HDM)

We consider a two-Higgs doublet model (2HDM) where an additional scalar doublet is introduced to the SM. The general scalar potential of the model is given as

$$\begin{aligned}
 V = & M_{11}^2 H_1^\dagger H_1 + M_{22}^2 H_2^\dagger H_2 - \left(M_{12}^2 H_1^\dagger H_2 + \text{h.c.} \right) \\
 & + \frac{\lambda_1}{2} (H_1^\dagger H_1)^2 + \frac{\lambda_2}{2} (H_2^\dagger H_2)^2 + \lambda_3 (H_1^\dagger H_1)(H_2^\dagger H_2) + \lambda_4 (H_1^\dagger H_2)(H_2^\dagger H_1) \\
 & + \frac{\lambda_5}{2} (H_1^\dagger H_2)^2 + \left\{ \lambda_6 (H_1^\dagger H_1) + \lambda_7 (H_2^\dagger H_2) \right\} (H_1^\dagger H_2) + \text{h.c.}
 \end{aligned} \quad (1)$$

Here, we work in the *Higgs basis* where only one doublet takes a VEV [93–95] at the renormalization scale $\mu = m_W$:

$$H_1 = \begin{pmatrix} G^+ \\ \frac{1}{\sqrt{2}}(v + h + iG^0) \end{pmatrix}, \quad H_2 = \begin{pmatrix} H^+ \\ \frac{1}{\sqrt{2}}(H + iA) \end{pmatrix}, \quad (2)$$

where $v \simeq 246 \text{ GeV}$ and G denotes the NG bosons.^{#1} The stationary conditions for Eq. (2) are

$$M_{11}^2 = -\frac{\lambda_1}{2}v^2, \quad M_{12}^2 = \frac{\lambda_6}{2}v^2. \quad (3)$$

We further assume the CP-conserving scalar potential, for simplicity. Then one can define the CP-even and -odd scalar mass eigenstates. The SM-like Higgs is h and a charged scalar is H^+ , while H and A correspond to additional CP-even and -odd neutral scalars.

It is noted that h - H mixing in their mass basis is suppressed as far as λ_6 is vanishing, so that all h interactions become the same as the SM Higgs boson at the renormalization scale $\mu = m_W$. This condition is known as the Higgs alignment limit [98–101]. In the following analysis, we assume $\lambda_6 = 0$ and consider phenomenology of the scalar bosons in the Higgs alignment limit. In this limit, scalar masses are related as

$$\begin{aligned}
 m_h^2 &= \lambda_1 v^2, \\
 m_{H^\pm}^2 &= M_{22}^2 + \frac{\lambda_3}{2}v^2, \\
 m_H^2 &= M_{22}^2 + \frac{\lambda_{hHH}}{2}v^2, \\
 m_A^2 &= M_{22}^2 + \frac{\lambda_{hAA}}{2}v^2.
 \end{aligned} \quad (4)$$

Here, for the latter convenience we defined

$$\lambda_{hHH} = \lambda_3 + \lambda_4 + \lambda_5, \quad \lambda_{hAA} = \lambda_3 + \lambda_4 - \lambda_5. \quad (5)$$

^{#1}Translation into the softly-broken \mathbb{Z}_2 symmetric Higgs potential with a finite $\tan\beta$ is possible, see Appendix of Refs. [96, 97].

The breakdown of the custodial symmetry is stringently constrained by measurements of the oblique parameters [102–104]. The constraint requires $m_H \simeq m_{H^\pm}$ or $m_A \simeq m_{H^\pm}$ to be consistent with the data [105]. This condition is equivalent to $\lambda_4 \simeq -\lambda_5$ or $\lambda_4 \simeq \lambda_5$, respectively. As seen in Eqs. (1) and (2), hHH and hAA couplings are controlled by λ_3 , λ_4 and λ_5 . The important point here is the sign in front of λ_5 . Since the λ_5 term in the potential is proportional to $(H_1^\dagger H_2)^2 + \text{h.c.}$, there is sign difference between hHH and hAA couplings. It is noted that hH^+H^- interaction is controlled by only λ_3 in the Higgs alignment limit.

We are interested in the di-Higgs production in the Higgs alignment limit. The production is relevant to Yukawa interactions. We define the Yukawa couplings involving extra scalars as follows [95]:

$$-\mathcal{L}_{H_2\text{-Yukawa}} = \overline{Q}^i \left(V_{\text{CKM}}^\dagger \right)^{ij} \tilde{H}_2 \rho_{jk}^u u_R^k + \overline{Q}^i H_2 \rho_{ij}^d d_R^j + \text{h.c.}, \quad (6)$$

with $\tilde{H}_2 = i\tau_2 H_2^*$ and focus on $\rho_{tt}^u \equiv \rho_{tt}^\phi$ interaction

$$-\mathcal{L}_{\text{Yukawa}}^t = \frac{\rho_{tt}^\phi}{\sqrt{2}} \bar{t} H t - i \frac{\rho_{tt}^\phi}{\sqrt{2}} \bar{t} A \gamma_5 t - \left[\rho_{tt}^\phi \bar{t}_R H^+ (V_{\text{CKM}} d_L)_3 + \text{h.c.} \right]. \quad (7)$$

We work in the down basis where the left-handed quarks are represented as $Q^T = \left(V_{\text{CKM}}^\dagger u_L \ d_L \right)$ with the mass eigenstates u_L and d_L .

Other Yukawa couplings, *e.g.*, tau Yukawa coupling will be introduced in the next section. The large additional top Yukawa coupling is realized in small β scenarios within the \mathbb{Z}_2 -based 2HDMs and a flavor-aligned 2HDM, for instance. In general ρ_{tt}^ϕ can be complex. Nevertheless, since the collider phenomenology below does not change in the presence of the phase in the Higgs alignment limit, and thus we omit it for simplicity. It is noted that if the additional bottom Yukawa coupling is sizable, the chirality enhanced amplitude significantly affects $b \rightarrow s\gamma$, and the scenario would be excluded easily. In the following, we label the additional lighter and heavier neutral scalars as ϕ_l and ϕ_h , respectively.

3 Phenomenology

In this section, we consider $h\phi_l$ production at the LHC. We evaluate the production cross section in Sec. 3.1 and discuss the phenomenological constraint on the relevant top Yukawa coupling in Sec. 3.2. The phenomenological impacts on the excesses are investigated in Sec. 3.3.

3.1 $h\phi_l$ production

In the SM, it is known that there is a partial cancellation among the diagrams in the Higgs pair production in the gluon-fusion processes [6, 7]. There are two types of the

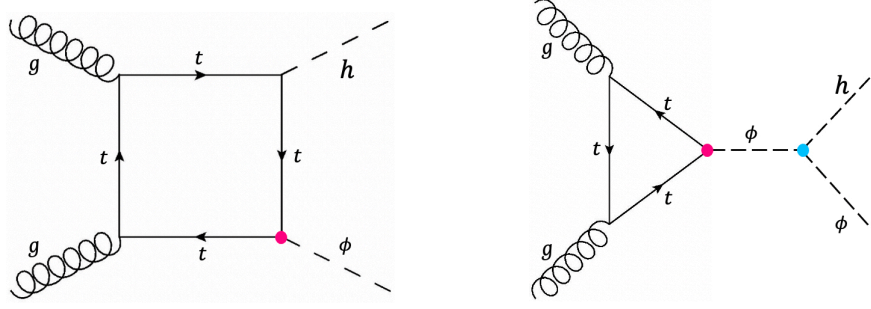


Figure 1. The representative Feynman diagrams for $h\phi$ production in the Higgs alignment limit, where $\phi = H$ or A is the additional scalar.

diagrams: one is the top box diagram and the other is the top triangle diagram with the triple Higgs coupling. Therefore, the modified triple Higgs coupling can be probed in this channel, and this process has eagerly been studied to test the structure of the Higgs potential.

In this work we extend this strategy to the $h\phi_l$ production. The representative Feynman diagrams for the scalar productions are shown in Fig. 1. The left and right diagrams show the top box and triangle induced contributions, respectively. The magenta vertex in the diagram corresponds to the additional top Yukawa coupling in Eq. (7), and the cyan one denotes the triple Higgs couplings. The previous data was not large enough to probe the new physics scenarios via this production when the additional scalar boson is heavy. However, the expected data at the current and future LHC can shed light on this production as we will show. Note that in the general 2HDM parameter space, for the $h\phi$ production there is another relevant diagram which comes from the Z -boson exchange Drell-Yan process. Although it is generated by the EW interaction, thanks to its tree-level nature, its contribution can be potentially much larger than the gluon-fusion process in Fig. 1 according to [89]. However, the important point is that such the EW production is significantly suppressed in the Higgs alignment limit, while the top loop induced productions are not suppressed.

As a demonstration, we consider a case of $\phi_l = A$ and $\phi_h = H$. We note that the CP-conserving scalar potential does not allow the hA production through $gg \rightarrow h$ or $H \rightarrow hA$. Furthermore in the Higgs alignment limit, $gg \rightarrow h \rightarrow hH$ vanishes. However, there is a non-vanishing triple Higgs coupling λ_{hAA} and hence $gg \rightarrow A \rightarrow hA$ process exists, as shown in Fig. 1.

In this study, there are four relevant free parameters to $h\phi_l$ production: (1) the produced scalar mass m_{ϕ_l} , (2) the heavier scalar mass m_{ϕ_h} , (3) the triple Higgs coupling λ_{hAA} (λ_{hHH}) for hA (hH) production, and (4) the additional top Yukawa coupling ρ_{tt}^ϕ . In our analysis, we fix m_{ϕ_l} and ρ_{tt}^ϕ and vary m_{ϕ_h} and λ_3 coupling with assuming $m_{H^\pm} = m_{\phi_h}$ to avoid the experimental bound from the oblique parameter. We numerically calculate the production cross section by MADGRAPH5_aMC@NLO [106] for a given set

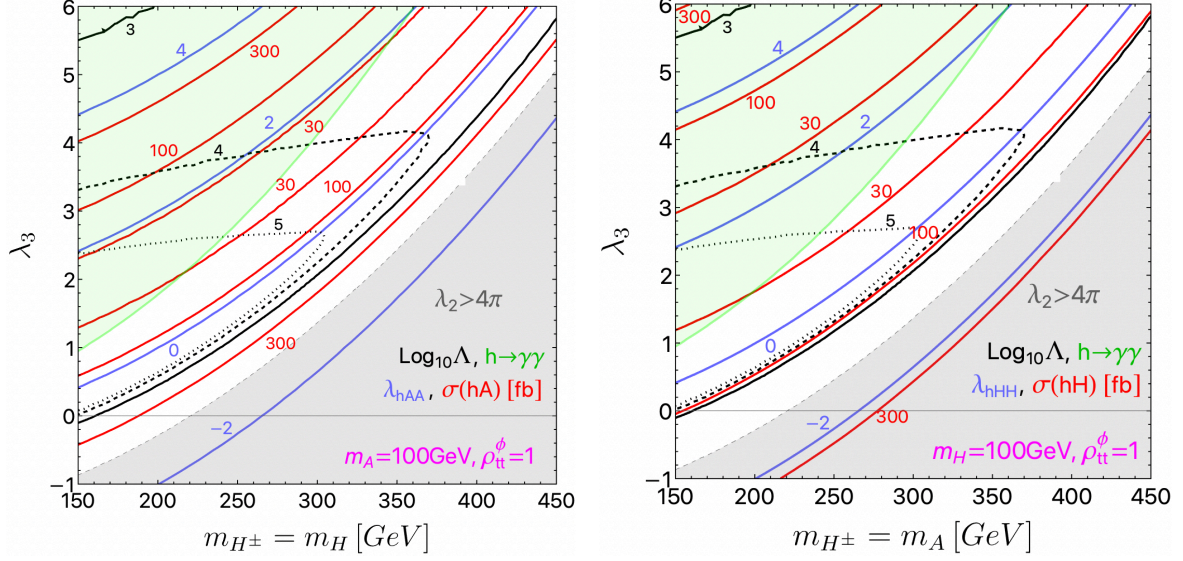


Figure 2. The $h\phi_l$ production cross section is shown in red contours on the heavier scalar mass and λ_3 plane. The lighter scalar mass is fixed as $m_A = 100$ GeV (left) and $m_H = 100$ GeV (right). The figures with other masses are found in Appendix A. Blue contours denote λ_{hAA} and λ_{hHH} at the additional scalar scale. The light green region and gray regions are excluded by the $h \rightarrow \gamma\gamma$ constraint and the vacuum stability condition, respectively. The black contours shows the cutoff scale in $\text{Log}_{10}(\Lambda/\text{GeV})$.

of A and H masses and λ_3 . 10K events are generated for each model point.^{#2} It is noted that the matrix elements of one-loop-induced $gg \rightarrow hA$ process have been validated against an independent implementation of 2HDM model in OPENLOOPS2 [108].

In Fig. 2, fixing $m_{\phi_l} = 100$ GeV, we show the $h\phi_l$ production cross section in the unit of fb and the $\lambda_{h\phi_l\phi_l}$ in red and blue contours, respectively. The result for $m_{\phi_l} = 50, 150, 200, 250, 300, 400$ GeV can be found in Appendix A. The vertical and horizontal axes correspond to λ_3 and m_{ϕ_h} . We set $\rho_{tt}^\phi = 1$ for simplicity since the both amplitudes corresponding to diagrams in Fig. 1 are linearly proportional to ρ_{tt}^ϕ . The cross section is proportional to $|\rho_{tt}^\phi|^2$, and thus it is easy to rescale the cross section.

Relevant constraints on ρ_{tt}^ϕ , which depends on scalar mass spectrum, are discussed in Sec. 3.2. Combining those constraints and production cross section in Figs. 2, 4 and 5, the realistic production cross section can be obtained. We observed that the SM-like destructive interference among the diagrams in Fig. 1 exists especially in the hA as well as hH production modes, where the additional γ_5 insertions play a similar role in the Dirac algebra of loop numerators in these diagrams. Our numerical analysis explicitly shows the destructive behavior in the parameter regions with $\lambda_{h\phi_l\phi_l} > 0$. It is observed that the production cross section can be $\mathcal{O}(100)$ fb for $m_{\phi_l} = 100$ GeV

^{#2}The numerical data of the production cross sections as well as the process and parameter cards for these analyses are available in the supplementary files in [107].

with $\rho_{tt}^\phi = 1$. For $m_{\phi_l} = 400$ GeV the cross section can be $\mathcal{O}(10)$ fb. We see that the cancellation occurs when $\lambda_{h\phi_l\phi_l}$ is of $\mathcal{O}(1)$.

Given the similarity between $h\phi$ production modes and the SM hh mode at the leading order and a fact that higher-order QCD corrections do not introduce additional γ_5 insertions, we expect a SM-like NLO QCD K -factor around 2 for the loop-induced $gg \rightarrow h\phi$ cross sections as well. This K -factor $\simeq 2$ is partially confirmed in Ref. [90] in the heavy top-mass limit, and it is important to confirm this expectation in the future by exact calculations which are out of the scope of this paper.

Furthermore, the Higgs precision data can constrain the parameter space. The one-loop induced charged scalar contribution modifies $h \rightarrow \gamma\gamma$ rate which has been measured with LHC Run 2 full data [109]. The light green region in Fig. 2 is excluded at the 2σ level. The constraint is especially relevant for the low-mass H^\pm region with large coupling λ_3 .

If the scalar couplings are too large, they eventually blow up at high energy because of the renormalization group evolution. We consider a perturbative unitarity bound [110–112] where the renormalization group evolution effect is considered based on Refs. [113, 114]. The black solid, dashed and dotted lines in Fig. 2 corresponds to the cutoff scale of $\Lambda = 10^3, 10^4$ and 10^5 GeV, respectively. If one requires that the model should be perturbative up to 10 TeV, the region outside the black dashed line will be discarded, for instance.

Another theoretical constraint on the quartic couplings comes from a vacuum stability of the scalar potential. In this paper, we impose the bounded-from-below condition at tree level. The bounded-from-below conditions for the scalar potential are [115, 116],

$$\lambda_1, \lambda_2 > 0, \quad 2\sqrt{\lambda_1\lambda_2} + \lambda_3 > 0, \quad 2\sqrt{\lambda_1\lambda_2} + \lambda_3 + \lambda_4 - |\lambda_5| > 0. \quad (8)$$

In order to produce a large mass difference between ϕ_l and ϕ_h , λ_4 must be largely negative value at the EW scale. Therefore, to satisfy the last condition in Eq. (8), λ_2 which does not change phenomenology must be largely positive. The gray region in Fig. 2 is excluded since there λ_2 becomes too large ($\lambda_2 > 4\pi$) to respect the bounded-from-below condition [117]. We see that various constraints are very complementary on this plane.

3.2 Constraints on ρ_{tt}^ϕ

In this section, we discuss relevant flavor and collider constraints on the scalar-top quark Yukawa couplings. First of all, we summarize the constraints from the direct searches at the LHC. The $t\bar{b}$ resonance search is relevant for H^\pm and the $t\bar{t}$ resonance searches are relevant for neutral scalars when ρ_{tt}^ϕ is dominant among the interactions. On the other hand, since a bound from the $\tau\bar{\tau}$ resonance search strongly depends on

whether the scalar has other decay modes or not, we consider only a case where ρ_{tt}^ϕ is dominant compared to other couplings, for simplicity.

In Fig. 3, we derive the upper limit on ρ_{tt}^ϕ as a function of $m_{H^\pm} (= m_{\phi_h})$. The orange region is excluded by $pp \rightarrow tbH^\pm \rightarrow \bar{t}b\bar{t}b$ process based on the LHC Run 2 full data [118] assuming $\text{BR}(H^\pm \rightarrow tb) = 1$. It is noted that the experimental data is available in the region of $m_{H^\pm} \geq 200$ GeV. In fact, there is also decay modes into gauge bosons, $H^\pm \rightarrow W^\pm \phi_l$ and the $\bar{t}b$ branching fraction is diluted for $m_{H^\pm} - m_{\phi_l} > m_W$. For instance, we obtain $\text{BR}(H^\pm \rightarrow tb) = 0.6$ for $\rho_{tt}^\phi = 1$ with $m_{H^\pm} = 350$ GeV and $m_{\phi_l} = 100$ GeV. Here, dilution of the bound significantly depends on m_{ϕ_l} .

Another collider constraint for a light H^\pm case could come from the exotic top decay which is available in the range of $m_{H^\pm} \leq 160$ GeV. If the couplings other than ρ_{tt}^ϕ are negligible for $m_{H^\pm} \leq m_t$, $H^\pm \rightarrow cb$ will be the dominant decay mode via ρ_{bb}^d or ρ_{tc}^u interactions in Eq. (6). Both ATLAS and CMS collaborations have searched for $H^\pm \rightarrow cb$ channel via a top quark decay [119, 120]. They set the upper limit on the product of $\text{BR}(t \rightarrow bH^\pm) \times \text{BR}(H^\pm \rightarrow bc)$ as a function of m_{H^\pm} . Assuming $\text{BR}(H^\pm \rightarrow cb) = 1$, we can set the upper limit on ρ_{tt}^ϕ which is shown by the blue region in Fig. 3. Similarly, if $H^\pm \rightarrow \tau\nu$ is the dominant decay mode via scalar-tau Yukawa interaction, we can set the upper limit on ρ_{tt}^ϕ which is shown by the purple region in Fig. 3 [121]. Furthermore, the similar upper limit can be obtained from $H^\pm \rightarrow cs$ via ρ_{cc}^u and ρ_{ss}^d [122]. It is noted that $t\bar{t}$ resonance and four-top searches give a weaker constraint [123], and thus are omitted.

The large ρ_{tt}^ϕ also modifies the $B_{(s)}$ -meson mixing, $\Delta M_{B_{(s)}}$ at one-loop level. We use the analytic formula for the H^\pm box contribution (H^\pm - W^\mp and H^\pm - H^\mp boxes) from Refs. [96, 124] and adopt the latest bound [125]. The renormalization group running correction from $\mu = m_{H^\pm}$ to $\mu = m_W$ is taken into account. Note that other flavor constraints, *e.g.*, from $b \rightarrow s\gamma$ and semileptonic decays of kaon are confirmed to be less stringent [126]. In Fig. 3, the light green region is excluded by the B_s mixing constraint. Since the B_s mixing constraint does not depend on m_{ϕ_l} and the decay modes, the bound is the most conservative in Fig. 3. It is observed that the mass gap exists for the LHC bounds around $m_{H^\pm} \sim m_t$ due to the experimental difficulty. However, the B_s mixing constraint is complementary and thus fills the gap.

It is observed that $\rho_{tt}^\phi \simeq 0.4$ is allowed for $m_{H^\pm} = 300$ GeV. Combining these constraints with Figs. 2, 4 and 5, one can read the maximal production cross section of the $h\phi_l$ channels.

It is worth mentioning that in addition to ρ_{tt}^ϕ bound, a severe constraint on $\lambda_{h\phi_l\phi_l}$ appears for $m_{\phi_l} \leq m_h/2$ in Fig. 4. In this parameter region, $h \rightarrow \phi_l\phi_l$ decay is kinematically open and modifies the Higgs total width. The partial decay width is given as

$$\Gamma(h \rightarrow \phi_l\phi_l) = \frac{\lambda_{h\phi_l\phi_l}^2 v^2}{32\pi m_h} \sqrt{1 - \frac{4m_{\phi_l}^2}{m_h^2}}. \quad (9)$$

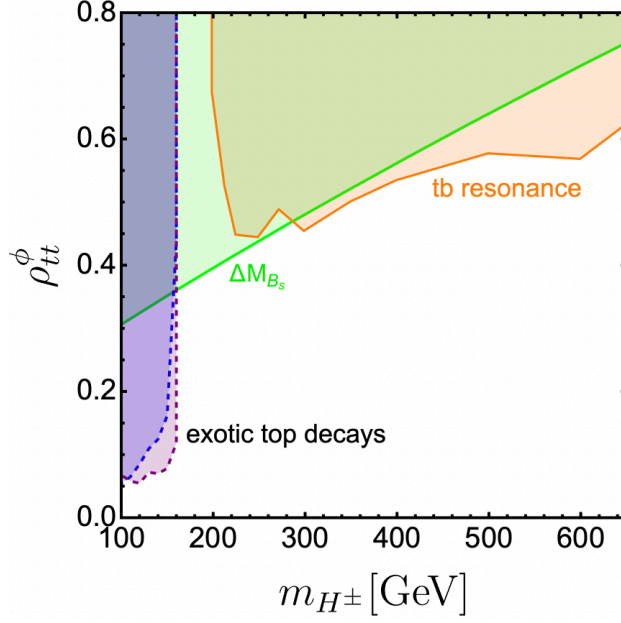


Figure 3. The upper limit on ρ_{tt}^ϕ as a function of m_{H^\pm} at 95% CL. Orange region is excluded by the tb resonance search. Purple and blue regions surrounded by dotted lines could be disfavored by the $t \rightarrow bH^\pm \rightarrow b\tau\nu$ and $t \rightarrow bH^\pm \rightarrow bbc$ decays, respectively. The light green region is excluded by the B_s -meson mixing bound.

The current bound [127, 128] corresponds to $\lambda_{h\phi_l\phi_l} \leq \mathcal{O}(10^{-2})$ for $m_{\phi_l} \leq m_h/2$.

3.3 Comment on solutions di- τ excess and muon $g - 2$

In this subsection we briefly discuss the phenomenological impacts on the di-tau excess and muon $g - 2$ anomaly solutions in the 2HDMs as an example.

Since the 100 GeV $\tau\bar{\tau}$ excess requires an additional light scalar decaying into di- τ final state, we introduce the following interaction,

$$-\mathcal{L}_{\text{Yukawa}}^\tau = \frac{\rho_{\tau\tau}^\phi}{\sqrt{2}} \bar{\tau} H \tau + i \frac{\rho_{\tau\tau}^\phi}{\sqrt{2}} \bar{\tau} A \gamma_5 \tau. \quad (10)$$

It is shown in Ref. [82] that a simultaneous explanation of the di-tau [79] and di-photon excesses [80] favors $m_{\phi_l} = m_A \simeq 95\text{--}100$ GeV with $\rho_{tt}^\phi \simeq 0.4$ and $\rho_{\tau\tau}^\phi \simeq 3 \times 10^{-3}$, which corresponds to $\text{BR}(A \rightarrow \tau\bar{\tau}) \simeq 0.3$. As seen from Fig. 3 that $m_{H^\pm} \leq 200$ GeV with $\rho_{tt}^\phi \simeq 0.4$ can not satisfy the ΔM_{B_s} bound. Furthermore, we found that $m_H \leq 2m_t$ is excluded by di- τ search [129].^{#3} For $m_H \geq 2m_t$, $\text{BR}(H \rightarrow \tau\bar{\tau})$ is significantly diluted and the bound becomes weak, so that the explanation is possible.

^{#3}It is noted that $m_{H^\pm} \leq m_t + m_b$ is also disfavored by the $\tau\nu$ resonance search associated with the top and bottom quarks [121].

On the other hand, the current 95% CL upper limits on the signal strengths of the di-Higgs production in $b\bar{b}\tau\bar{\tau}$ decay mode is given as $\mu(hh \rightarrow b\bar{b}\tau\bar{\tau}) \leq 3.3$ [130]. The NNLO SM prediction is given as $\sigma_{\text{ggF}}^{hh} = 31.05_{-23\%}^{+6\%} \pm 3\%$ fb with $m_h = 125$ GeV [23, 131]. It is noted that the experimental upper limit is a consequence of the combination of gluon fusion (ggF) and vector boson fusion (VBF). Although the VBF cross section is small, $\sigma_{\text{VBF}}^{hh} = 1.73_{-0.04\%}^{+0.03\%} \pm 2.1\%$ fb at NNLO [131], the unique VBF event topology provides a useful handle to identify signal events and sensitivity. Although it is nontrivial to separate the impacts of ggF and VBF determination, the ggF mainly determine the upper limit [130]. Using the SM predictions $\text{BR}(h \rightarrow b\bar{b}) = 58.1\%$ and $\text{BR}(h \rightarrow \tau\bar{\tau}) = 6.3\%$, and if we estimate a rough sensitivity by only considering the ggF mode, the current LHC data reaches 7.5 fb for the di-Higgs production with $b\bar{b}\tau\bar{\tau}$ final state.

We see from Fig. 2 that $\sigma(pp \rightarrow hA)$ is as large as 200 fb for $\rho_{tt}^\phi = 1$ when the cutoff scale $\Lambda > 10$ TeV is imposed. For $\rho_{tt}^\phi = 0.4$, the production cross section is calculated as $\sigma(pp \rightarrow hA) = 200 \times 0.4^2 \simeq 30$ fb. Therefore the explanation of $\tau\bar{\tau}$ excess with $m_A \sim 100$ GeV, $\rho_{tt}^\phi = 0.4$, $\rho_{\tau\tau}^\phi = 3 \times 10^{-3}$ predicts $\sigma(pp \rightarrow hA) \times \text{BR}(h \rightarrow b\bar{b}) \times \text{BR}(A \rightarrow \tau\bar{\tau}) \simeq 5.6$ fb that is larger than the SM di-Higgs prediction (2.3 fb). If the K -factor is about 2 for $\sigma(pp \rightarrow hA)$, the model prediction exceeds the current exclusion for the hh channel. It is shown in Ref. [82], unlike the CP-even interpretation, it is challenging to test the CP-odd solution for the $\tau\bar{\tau}$ excess in $t\bar{t} + \tau\bar{\tau}$ final state. On the other hand, the hA production (decaying into $b\bar{b}\tau\bar{\tau}$) allows us probe the solution. However, the more dedicated sensitivity study is necessary from both experimental and theoretical sides due to $m_A \neq m_h$. It is noted that the single H production process can be relevant for the model parameter set. The CMS collaboration probed $pp \rightarrow H \rightarrow AZ \rightarrow \tau\bar{\tau} + l\bar{l}$ process with the Run 1 data and the $\mathcal{O}(10)$ fb upper limit on $\sigma(pp \rightarrow H \rightarrow AZ \rightarrow \tau\bar{\tau} + l\bar{l})$ has been set.^{#4} We calculated the signal cross section based on the SUSHi [134, 135] and confirmed that the parameter predicts the smaller signal cross section by roughly a factor of 1/2. The LHC Run 2 full result would give conclusive evidences.

It is known that a light pseudo scalar is necessary for an explanation of the muon $g - 2$ anomaly in the type-X and flavor-aligned (FA) 2HDMs [78], where the dominant contribution comes from Barr-Zee two-loop diagram with tau loop. In the type-X 2HDM, the top Yukawa coupling with the heavy scalar is $\mathcal{O}(0.01)$ for the excess favored region. Therefore, the di-Higgs production cross section is too small to be observed. We also found that even in the FA2HDM, the top Yukawa coupling can not be large due to the constraint from $B_s \rightarrow \mu\bar{\mu}$ measurement that is enhanced with a light scalar exchange diagram [136]. Furthermore, it would not be easy to reconstruct the additional light scalar in $\tau\bar{\tau}$ final state at the LHC due to several neutrinos. Therefore, we conclude that the di-Higgs production for the solution of the muon $g - 2$ anomaly

^{#4}The ATLAS and CMS collaborations focused on only $b\bar{b} + l\bar{l}$ final state in the Run 2 data [132, 133].

is less relevant.

4 Conclusion

The Higgs field plays a very important role in giving the mass to the SM particles. However, there are still open questions, *e.g.*, the origins of the negative mass term and hierarchy of the fermions. There would be new physics to solve the questions. On the other hand, it is known that the extended Higgs models can be the key to explain the origins of the neutrino masses, EW baryogenesis, dark matter and vacuum stability. Therefore it is often believed that study of the Higgs sector is the way to access physics beyond the SM. The 2HDM is one of the simplest extensions of the SM that frequently appears in the new physics scenarios. It is known that this model can explain the excesses in the $\tau\bar{\tau}$ and $\gamma\gamma$ resonances data reported by the CMS collaboration as well as the muon $g - 2$ discrepancy. Those discrepancies require a light neutral scalar which will be within the reach of the LHC. This kind of light scalar is also well motivated by a successful strong first-order EW phase transition and the baryon asymmetry of the universe.

In order to chase a realistic and still-allowed 2HDM that can resolve the aforementioned puzzles, in this paper we investigated the $h\phi$ production where ϕ is the additional neutral scalar ($\phi = H, A$). This process will be interesting in the HL-LHC era. We calculated the cross section of $h\phi$ production from the loop-induced gluon fusion channel at the leading order. We took into account the theoretical bounds from the perturbative unitarity and vacuum stability conditions, the precision measurements from the Higgs and flavor physics, and the direct search constraints. It is found that $h\phi$ production cross section could be as large as $\mathcal{O}(30)$ fb if the additional scalar mass is around 100 GeV.

Furthermore, motivated by the low mass $\tau\bar{\tau}$ and $\gamma\gamma$ resonant excesses reported by the CMS collaboration, the impact of the $h\phi$ production is investigated. It was found that the combined explanation of the excesses predicts $\sigma(pp \rightarrow hA \rightarrow b\bar{b}\tau\bar{\tau}) \simeq 6$ fb. Very interestingly, this leading-order cross section is already larger than the SM Higgs-pair production decaying into $b\bar{b}\tau\bar{\tau}$ by a factor of more than 2. Therefore, this mode provides a unique window to probe the possible explanation of the excesses. At last, it is clear that more dedicated precise calculations and experimental simulation to evaluate the realistic sensitivity are further needed.

Acknowledgements

The authors would like to thank Sven Heinemeyer, Jonas Lindert, Ulrich Nierste, Masanori Tanaka, and Kei Yagyu for fruitful comments and valuable discussion. S.I.

and T. K. thank the workshop “Physics in LHC and Beyond”, where a part of discussion took place. We also appreciate TTP KIT for the massive computational support, especially we thank Martin Lang, Fabian Lange and Kay Schönwald for the computational help. S. I. and H. Z. are supported by the Deutsche Forschungsgemeinschaft (DFG, German Research Foundation) under grant 396021762-TRR 257. T. K. is supported by the Grant-in-Aid for Early-Career Scientists from the Ministry of Education, Culture, Sports, Science, and Technology (MEXT), Japan, No. 19K14706. The work of Y. O. is supported by Grant-in-Aid for Scientific research from the MEXT, Japan, No. 19K03867. This work is also supported by the Japan Society for the Promotion of Science (JSPS) Core-to-Core Program, No. JPJSCCA20200002.

A Additional figures

In this Appendix, we present figures that are not shown in the main text. Figure 4 shows the production cross sections for $m_{\phi_l} = 50$ GeV (upper), 150 GeV (middle) and 200 GeV (bottom). Figure 5 shows the results for $m_{\phi_l} = 250$ GeV (upper), 300 GeV (middle) and 400 GeV (bottom). The color code is the same as Fig. 2 and for the description of the contours see the caption of Fig. 2 and the main text. For $m_{\phi_l} = 50$ GeV, the Higgs width bound gives a stringent constraint on $\lambda_{h\phi_l\phi_l}$ since $h \rightarrow \phi_l\phi_l$ is kinematically open. Therefore, the allowed region from the Higgs width bound is almost degenerated to the line of $\lambda_{h\phi_l\phi_l} = 0$. It is noted that the constraint from $h \rightarrow \gamma\gamma$ does not appear on the plane with $m_{\phi_l} = 400$ GeV. As mentioned in Sec. 3.1, the cross section data is available in [107].

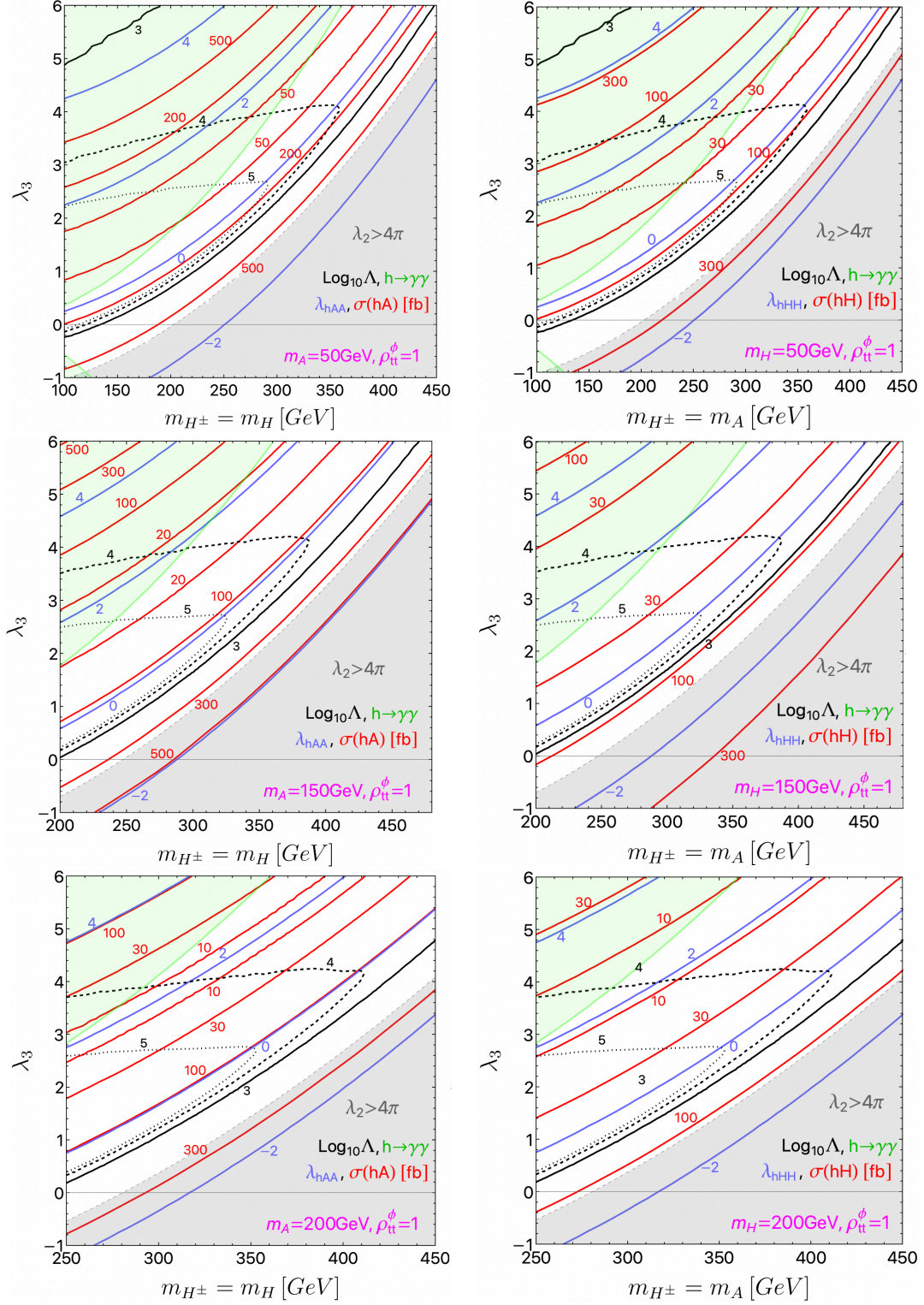


Figure 4. The $h\phi_l$ production cross section is shown on the heavier scalar mass vs. λ_3 plane. The left and right figures are for hA and hH productions, respectively. The lighter scalar mass is fixed to be 50 GeV (upper), 150 GeV (middle), 200 GeV (bottom). See, the caption of Fig. 2 for the description of the constraints and other explanations.

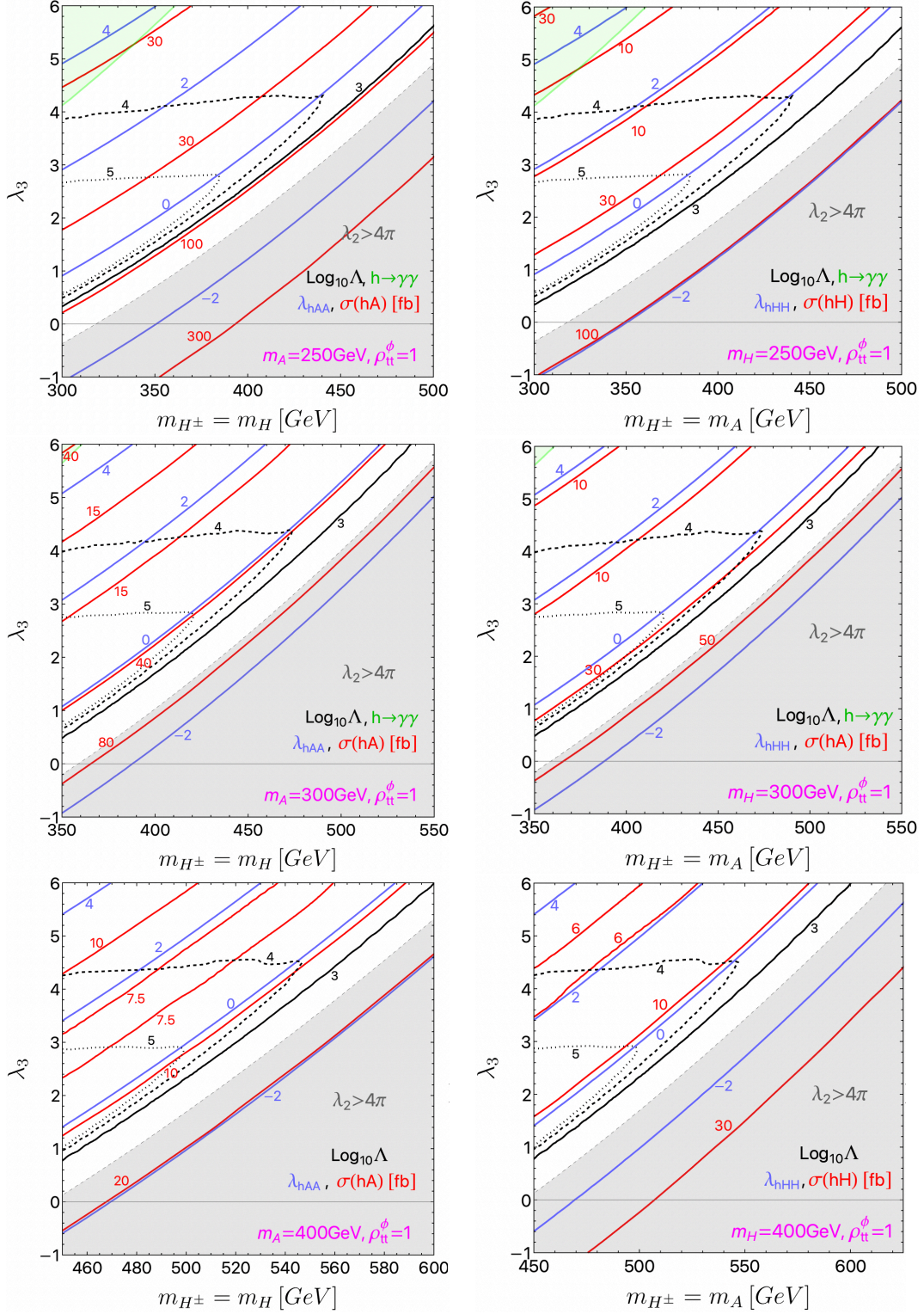


Figure 5. The $h\phi_l$ production cross section is shown on the heavier scalar mass vs. λ_3 plane. The left and right figures are for hA and hH productions, respectively. The lighter scalar mass is fixed to be 250 GeV (upper), 300 GeV (middle), 400 GeV (bottom). See, the caption of Fig. 2 for the description of the constraints and other explanations.

References

- [1] S. L. Glashow, “Partial Symmetries of Weak Interactions,” *Nucl. Phys.* **22** (1961) 579–588.
- [2] J. Goldstone, A. Salam, and S. Weinberg, “Broken Symmetries,” *Phys. Rev.* **127** (1962) 965–970.
- [3] P. W. Higgs, “Broken Symmetries and the Masses of Gauge Bosons,” *Phys. Rev. Lett.* **13** (1964) 508–509.
- [4] F. Englert and R. Brout, “Broken Symmetry and the Mass of Gauge Vector Mesons,” *Phys. Rev. Lett.* **13** (1964) 321–323.
- [5] G. S. Guralnik, C. R. Hagen, and T. W. B. Kibble, “Global Conservation Laws and Massless Particles,” *Phys. Rev. Lett.* **13** (1964) 585–587.
- [6] **LHC Higgs Cross Section Working Group** Collaboration, “Handbook of LHC Higgs Cross Sections: 4. Deciphering the Nature of the Higgs Sector.” [arXiv:1610.07922](#).
- [7] M. Cepeda *et al.*, “Report from Working Group 2: Higgs Physics at the HL-LHC and HE-LHC,” *CERN Yellow Rep. Monogr.* **7** (2019) 221–584 [[arXiv:1902.00134](#)].
- [8] S. Dawson, S. Dittmaier, and M. Spira, “Neutral Higgs boson pair production at hadron colliders: QCD corrections,” *Phys. Rev. D* **58** (1998) 115012 [[hep-ph/9805244](#)].
- [9] J. Grigo, J. Hoff, K. Melnikov, and M. Steinhauser, “On the Higgs boson pair production at the LHC,” *Nucl. Phys. B* **875** (2013) 1–17 [[arXiv:1305.7340](#)].
- [10] S. Borowka, *et al.*, “Higgs Boson Pair Production in Gluon Fusion at Next-to-Leading Order with Full Top-Quark Mass Dependence,” *Phys. Rev. Lett.* **117** (2016) 012001 [[arXiv:1604.06447](#)]. [Erratum: *Phys.Rev.Lett.* 117, 079901 (2016)].
- [11] S. Borowka, *et al.*, “Full top quark mass dependence in Higgs boson pair production at NLO,” *JHEP* **10** (2016) 107 [[arXiv:1608.04798](#)].
- [12] R. Gröber, A. Maier, and T. Rauh, “Reconstruction of top-quark mass effects in Higgs pair production and other gluon-fusion processes,” *JHEP* **03** (2018) 020 [[arXiv:1709.07799](#)].
- [13] J. Baglio, *et al.*, “Gluon fusion into Higgs pairs at NLO QCD and the top mass scheme,” *Eur. Phys. J. C* **79** (2019) 459 [[arXiv:1811.05692](#)].
- [14] J. Davies, G. Mishima, M. Steinhauser, and D. Wellmann, “Double Higgs boson production at NLO in the high-energy limit: complete analytic results,” *JHEP* **01** (2019) 176 [[arXiv:1811.05489](#)].
- [15] R. Bonciani, G. Degrandi, P. P. Giardino, and R. Gröber, “Analytical Method for Next-to-Leading-Order QCD Corrections to Double-Higgs Production,” *Phys. Rev. Lett.* **121** (2018) 162003 [[arXiv:1806.11564](#)].
- [16] X. Xu and L. L. Yang, “Towards a new approximation for pair-production and associated-production of the Higgs boson,” *JHEP* **01** (2019) 211 [[arXiv:1810.12002](#)].
- [17] J. Davies, *et al.*, “Double Higgs boson production at NLO: combining the exact numerical result and high-energy expansion,” *JHEP* **11** (2019) 024 [[arXiv:1907.06408](#)].
- [18] L. Bellafronte, G. Degrandi, P. P. Giardino, R. Gröber, and M. Vitti, “Gluon fusion production at NLO: merging the transverse momentum and the high-energy expansions,” *JHEP* **07** (2022) 069 [[arXiv:2202.12157](#)].

- [19] D. de Florian and J. Mazzitelli, “Higgs Boson Pair Production at Next-to-Next-to-Leading Order in QCD,” *Phys. Rev. Lett.* **111** (2013) 201801 [[arXiv:1309.6594](#)].
- [20] D. de Florian and J. Mazzitelli, “Two-loop virtual corrections to Higgs pair production,” *Phys. Lett. B* **724** (2013) 306–309 [[arXiv:1305.5206](#)].
- [21] J. Grigo, J. Hoff, and M. Steinhauser, “Higgs boson pair production: top quark mass effects at NLO and NNLO,” *Nucl. Phys. B* **900** (2015) 412–430 [[arXiv:1508.00909](#)].
- [22] M. Spira, “Effective Multi-Higgs Couplings to Gluons,” *JHEP* **10** (2016) 026 [[arXiv:1607.05548](#)].
- [23] M. Grazzini, *et al.*, “Higgs boson pair production at NNLO with top quark mass effects,” *JHEP* **05** (2018) 059 [[arXiv:1803.02463](#)].
- [24] M. Gerlach, F. Herren, and M. Steinhauser, “Wilson coefficients for Higgs boson production and decoupling relations to $\mathcal{O}(\alpha_s^4)$,” *JHEP* **11** (2018) 141 [[arXiv:1809.06787](#)].
- [25] L.-B. Chen, H. T. Li, H.-S. Shao, and J. Wang, “The gluon-fusion production of Higgs boson pair: N³LO QCD corrections and top-quark mass effects,” *JHEP* **03** (2020) 072 [[arXiv:1912.13001](#)].
- [26] J. Davies, F. Herren, G. Mishima, and M. Steinhauser, “Real-virtual corrections to Higgs boson pair production at NNLO: three closed top quark loops,” *JHEP* **05** (2019) 157 [[arXiv:1904.11998](#)].
- [27] J. Davies, F. Herren, G. Mishima, and M. Steinhauser, “Real corrections to Higgs boson pair production at NNLO in the large top quark mass limit,” *JHEP* **01** (2022) 049 [[arXiv:2110.03697](#)].
- [28] A. H. Ajjath and H.-S. Shao, “N³LO+N³LL QCD improved Higgs pair cross sections.” [arXiv:2209.03914](#).
- [29] J. Davies, G. Mishima, K. Schönwald, M. Steinhauser, and H. Zhang, “Higgs boson contribution to the leading two-loop Yukawa corrections to $gg \rightarrow HH$,” *JHEP* **08** (2022) 259 [[arXiv:2207.02587](#)].
- [30] M. Mühlleitner, J. Schlenk, and M. Spira, “Top-Yukawa-induced Corrections to Higgs Pair Production.” [arXiv:2207.02524](#).
- [31] **ATLAS** Collaboration, “The ATLAS Experiment at the CERN Large Hadron Collider,” *JINST* **3** (2008) S08003.
- [32] **CMS** Collaboration, “The CMS Experiment at the CERN LHC,” *JINST* **3** (2008) S08004.
- [33] **CMS** Collaboration, “Performance of reconstruction and identification of τ leptons decaying to hadrons and ν_τ in pp collisions at $\sqrt{s} = 13$ TeV,” *JINST* **13** (2018) P10005 [[arXiv:1809.02816](#)].
- [34] **ATLAS** Collaboration, “ATLAS b-jet identification performance and efficiency measurement with $t\bar{t}$ events in pp collisions at $\sqrt{s} = 13$ TeV,” *Eur. Phys. J. C* **79** (2019) 970 [[arXiv:1907.05120](#)].
- [35] **CMS** Collaboration, “Search for Higgs boson pair production in events with two bottom quarks and two tau leptons in proton–proton collisions at $\sqrt{s} = 13$ TeV,” *Phys. Lett. B* **778** (2018) 101–127 [[arXiv:1707.02909](#)].

- [36] CMS Collaboration, “Search for resonant and nonresonant Higgs boson pair production in the $b\bar{b}\ell\nu\ell\nu$ final state in proton-proton collisions at $\sqrt{s} = 13$ TeV,” *JHEP* **01** (2018) 054 [[arXiv:1708.04188](#)].
- [37] ATLAS Collaboration, “Search for pair production of Higgs bosons in the $b\bar{b}b\bar{b}$ final state using proton-proton collisions at $\sqrt{s} = 13$ TeV with the ATLAS detector,” *JHEP* **01** (2019) 030 [[arXiv:1804.06174](#)].
- [38] ATLAS Collaboration, “Search for Higgs boson pair production in the $\gamma\gamma b\bar{b}$ final state with 13 TeV pp collision data collected by the ATLAS experiment,” *JHEP* **11** (2018) 040 [[arXiv:1807.04873](#)].
- [39] ATLAS Collaboration, “Search for resonant and non-resonant Higgs boson pair production in the $b\bar{b}\tau^+\tau^-$ decay channel in pp collisions at $\sqrt{s} = 13$ TeV with the ATLAS detector,” *Phys. Rev. Lett.* **121** (2018) 191801 [[arXiv:1808.00336](#)]. [Erratum: *Phys. Rev. Lett.* **122**, 089901 (2019)].
- [40] CMS Collaboration, “Search for nonresonant Higgs boson pair production in the $b\bar{b}b\bar{b}$ final state at $\sqrt{s} = 13$ TeV,” *JHEP* **04** (2019) 112 [[arXiv:1810.11854](#)].
- [41] ATLAS Collaboration, “Search for Higgs boson pair production in the $b\bar{b}WW^*$ decay mode at $\sqrt{s} = 13$ TeV with the ATLAS detector,” *JHEP* **04** (2019) 092 [[arXiv:1811.04671](#)].
- [42] ATLAS Collaboration, “Search for non-resonant Higgs boson pair production in the $b\bar{b}\ell\nu\ell\nu$ final state with the ATLAS detector in pp collisions at $\sqrt{s} = 13$ TeV,” *Phys. Lett. B* **801** (2020) 135145 [[arXiv:1908.06765](#)].
- [43] CMS Collaboration, “Search for nonresonant Higgs boson pair production in final states with two bottom quarks and two photons in proton-proton collisions at $\sqrt{s} = 13$ TeV,” *JHEP* **03** (2021) 257 [[arXiv:2011.12373](#)].
- [44] ATLAS Collaboration, “Search for Higgs boson pair production in the two bottom quarks plus two photons final state in pp collisions at $\sqrt{s} = 13$ TeV with the ATLAS detector,” *Phys. Rev. D* **106** (2022) 052001 [[arXiv:2112.11876](#)].
- [45] CMS Collaboration, “Search for Higgs Boson Pair Production in the Four b Quark Final State in Proton-Proton Collisions at $\sqrt{s} = 13$ TeV,” *Phys. Rev. Lett.* **129** (2022) 081802 [[arXiv:2202.09617](#)].
- [46] ATLAS Collaboration, “Search for resonant and non-resonant Higgs boson pair production in the $b\bar{b}\tau^+\tau^-$ decay channel using 13 TeV pp collision data from the ATLAS detector.” [[arXiv:2209.10910](#)].
- [47] ATLAS Collaboration, “Measurement prospects of Higgs boson pair production in the $b\bar{b}\gamma\gamma$ final state with the ATLAS experiment at the HL-LHC.” [<http://cds.cern.ch/record/2799146>].
- [48] S. P. Martin, “A Supersymmetry primer,” *Adv. Ser. Direct. High Energy Phys.* **18** (1998) 1–98 [[hep-ph/9709356](#)].
- [49] G. Degrandi, S. Heinemeyer, W. Hollik, P. Slavich, and G. Weiglein, “Towards high precision predictions for the MSSM Higgs sector,” *Eur. Phys. J. C* **28** (2003) 133–143 [[hep-ph/0212020](#)].
- [50] R. N. Mohapatra and J. C. Pati, “A Natural Left-Right Symmetry,” *Phys. Rev. D* **11** (1975) 2558.

- [51] **ATLAS** Collaboration, “Observation of a new particle in the search for the Standard Model Higgs boson with the ATLAS detector at the LHC,” *Phys. Lett. B* **716** (2012) 1–29 [[arXiv:1207.7214](#)].
- [52] **CMS** Collaboration, “Observation of a New Boson at a Mass of 125 GeV with the CMS Experiment at the LHC,” *Phys. Lett. B* **716** (2012) 30–61 [[arXiv:1207.7235](#)].
- [53] **ATLAS, CMS** Collaboration, “Measurements of the Higgs boson production and decay rates and constraints on its couplings from a combined ATLAS and CMS analysis of the LHC pp collision data at $\sqrt{s} = 7$ and 8 TeV,” *JHEP* **08** (2016) 045 [[arXiv:1606.02266](#)].
- [54] **ATLAS** Collaboration, “A detailed map of Higgs boson interactions by the ATLAS experiment ten years after the discovery,” *Nature* **607** (2022) 52–59 [[arXiv:2207.00092](#)].
- [55] J. M. Cline, “Baryogenesis,” in *Les Houches Summer School - Session 86: Particle Physics and Cosmology: The Fabric of Spacetime*. 2006. [hep-ph/0609145](#).
- [56] J. M. Cline, K. Kainulainen, and A. P. Vischer, “Dynamics of two Higgs doublet CP violation and baryogenesis at the electroweak phase transition,” *Phys. Rev. D* **54** (1996) 2451–2472 [[hep-ph/9506284](#)].
- [57] N. Turok and J. Zadrozny, “Electroweak baryogenesis in the two doublet model,” *Nucl. Phys. B* **358** (1991) 471–493.
- [58] N. Turok and J. Zadrozny, “Phase transitions in the two doublet model,” *Nucl. Phys. B* **369** (1992) 729–742.
- [59] S. Kanemura and M. Tanaka, “Strongly first-order electroweak phase transition by relatively heavy additional Higgs bosons,” *Phys. Rev. D* **106** (2022) 035012 [[arXiv:2201.04791](#)].
- [60] K. Fuyuto, W.-S. Hou, and E. Senaha, “Electroweak baryogenesis driven by extra top Yukawa couplings,” *Phys. Lett. B* **776** (2018) 402–406 [[arXiv:1705.05034](#)].
- [61] E. Ma, “Verifiable radiative seesaw mechanism of neutrino mass and dark matter,” *Phys. Rev. D* **73** (2006) 077301 [[hep-ph/0601225](#)].
- [62] M. Aoki, S. Kanemura, and O. Seto, “Neutrino mass, Dark Matter and Baryon Asymmetry via TeV-Scale Physics without Fine-Tuning,” *Phys. Rev. Lett.* **102** (2009) 051805 [[arXiv:0807.0361](#)].
- [63] A. Ahriche, A. Jueid, and S. Nasri, “Radiative neutrino mass and Majorana dark matter within an inert Higgs doublet model,” *Phys. Rev. D* **97** (2018) 095012 [[arXiv:1710.03824](#)].
- [64] T. Aoyama *et al.*, “The anomalous magnetic moment of the muon in the Standard Model,” *Phys. Rept.* **887** (2020) 1–166 [[arXiv:2006.04822](#)].
- [65] **Muon g-2** Collaboration, “Final Report of the Muon E821 Anomalous Magnetic Moment Measurement at BNL,” *Phys. Rev. D* **73** (2006) 072003 [[hep-ex/0602035](#)].
- [66] **Muon g-2** Collaboration, “Precise measurement of the positive muon anomalous magnetic moment,” *Phys. Rev. Lett.* **86** (2001) 2227–2231 [[hep-ex/0102017](#)].
- [67] **Muon g-2** Collaboration, “Measurement of the Positive Muon Anomalous Magnetic Moment to 0.46 ppm,” *Phys. Rev. Lett.* **126** (2021) 141801 [[arXiv:2104.03281](#)].
- [68] **RBC, UKQCD** Collaboration, “Calculation of the hadronic vacuum polarization contribution to the muon anomalous magnetic moment,” *Phys. Rev. Lett.* **121** (2018) 022003 [[arXiv:1801.07224](#)].

- [69] S. Borsanyi *et al.*, “Leading hadronic contribution to the muon magnetic moment from lattice QCD,” *Nature* **593** (2021) 51–55 [[arXiv:2002.12347](#)].
- [70] C. Lehner and A. S. Meyer, “Consistency of hadronic vacuum polarization between lattice QCD and the R-ratio,” *Phys. Rev. D* **101** (2020) 074515 [[arXiv:2003.04177](#)].
- [71] **chiQCD** Collaboration, “Muon $g-2$ with overlap valence fermion.” [arXiv:2204.01280](#).
- [72] C. Aubin, T. Blum, M. Golterman, and S. Peris, “Muon anomalous magnetic moment with staggered fermions: Is the lattice spacing small enough?” *Phys. Rev. D* **106** (2022) 054503 [[arXiv:2204.12256](#)].
- [73] M. Cè *et al.*, “Window observable for the hadronic vacuum polarization contribution to the muon $g - 2$ from lattice QCD.” [arXiv:2206.06582](#).
- [74] C. Alexandrou *et al.*, “Lattice calculation of the short and intermediate time-distance hadronic vacuum polarization contributions to the muon magnetic moment using twisted-mass fermions.” [arXiv:2206.15084](#).
- [75] A. Crivellin, M. Hoferichter, C. A. Manzari, and M. Montull, “Hadronic Vacuum Polarization: $(g - 2)_\mu$ versus Global Electroweak Fits,” *Phys. Rev. Lett.* **125** (2020) 091801 [[arXiv:2003.04886](#)].
- [76] A. Keshavarzi, W. J. Marciano, M. Passera, and A. Sirlin, “Muon $g - 2$ and $\Delta\alpha$ connection,” *Phys. Rev. D* **102** (2020) 033002 [[arXiv:2006.12666](#)].
- [77] G. Colangelo, M. Hoferichter, and P. Stoffer, “Constraints on the two-pion contribution to hadronic vacuum polarization,” *Phys. Lett. B* **814** (2021) 136073 [[arXiv:2010.07943](#)].
- [78] P. M. Ferreira, B. L. Gonçalves, F. R. Joaquim, and M. Sher, “ $(g - 2)_\mu$ in the 2HDM and slightly beyond: An updated view,” *Phys. Rev. D* **104** (2021) 053008 [[arXiv:2104.03367](#)].
- [79] **CMS** Collaboration, “Searches for additional Higgs bosons and for vector leptoquarks in $\tau\tau$ final states in proton-proton collisions at $\sqrt{s} = 13$ TeV.” [arXiv:2208.02717](#).
- [80] **CMS** Collaboration, “Search for a standard model-like Higgs boson in the mass range between 70 and 110 GeV in the diphoton final state in proton-proton collisions at $\sqrt{s} = 8$ and 13 TeV,” *Phys. Lett. B* **793** (2019) 320–347 [[arXiv:1811.08459](#)].
- [81] **LEP Working Group for Higgs boson searches, ALEPH, DELPHI, L3, OPAL** Collaboration, “Search for the standard model Higgs boson at LEP,” *Phys. Lett. B* **565** (2003) 61–75 [[hep-ex/0306033](#)].
- [82] S. Iguro, T. Kitahara, and Y. Omura, “Scrutinizing the 95-100 GeV di-tau excess in the top associated process.” [arXiv:2205.03187](#).
- [83] T. Plehn, M. Spira, and P. M. Zerwas, “Pair production of neutral Higgs particles in gluon-gluon collisions,” *Nucl. Phys. B* **479** (1996) 46–64 [[hep-ph/9603205](#)]. [Erratum: *Nucl.Phys.B* 531, 655–655 (1998)].
- [84] A. Djouadi, W. Kilian, M. Muhlleitner, and P. M. Zerwas, “Production of neutral Higgs boson pairs at LHC,” *Eur. Phys. J. C* **10** (1999) 45–49 [[hep-ph/9904287](#)].
- [85] A. Arhrib, R. Benbrik, R. B. Guedes, and R. Santos, “Search for a light fermiophobic Higgs boson produced via gluon fusion at Hadron Colliders,” *Phys. Rev. D* **78** (2008) 075002 [[arXiv:0805.1603](#)].

- [86] A. Arhrib, R. Benbrik, C.-H. Chen, R. Guedes, and R. Santos, “Double Neutral Higgs production in the Two-Higgs doublet model at the LHC,” *JHEP* **08** (2009) 035 [[arXiv:0906.0387](#)].
- [87] M. J. Dolan, C. Englert, and M. Spannowsky, “New Physics in LHC Higgs boson pair production,” *Phys. Rev. D* **87** (2013) 055002 [[arXiv:1210.8166](#)].
- [88] B. Hespel, D. Lopez-Val, and E. Vryonidou, “Higgs pair production via gluon fusion in the Two-Higgs-Doublet Model,” *JHEP* **09** (2014) 124 [[arXiv:1407.0281](#)].
- [89] R. Enberg, W. Klemm, S. Moretti, and S. Munir, “Electroweak production of light scalar–pseudoscalar pairs from extended Higgs sectors,” *Phys. Lett. B* **764** (2017) 121–125 [[arXiv:1605.02498](#)].
- [90] H. Abouabid, *et al.*, “Benchmarking di-Higgs production in various extended Higgs sector models,” *JHEP* **09** (2022) 011 [[arXiv:2112.12515](#)].
- [91] H.-Y. Li, *et al.*, “Scalar-pseudoscalar pair production at the Large Hadron Collider at NLO+NLL accuracy in QCD *,” *Chin. Phys. C* **45** (2021) 123102 [[arXiv:2112.13337](#)].
- [92] H. Bahl, *et al.*, “HiggsTools: BSM scalar phenomenology with new versions of HiggsBounds and HiggsSignals.” [arXiv:2210.09332](#).
- [93] H. Georgi and D. V. Nanopoulos, “Suppression of Flavor Changing Effects From Neutral Spinless Meson Exchange in Gauge Theories,” *Phys. Lett. B* **82** (1979) 95–96.
- [94] J. F. Donoghue and L. F. Li, “Properties of Charged Higgs Bosons,” *Phys. Rev. D* **19** (1979) 945.
- [95] S. Davidson and H. E. Haber, “Basis-independent methods for the two-Higgs-doublet model,” *Phys. Rev. D* **72** (2005) 035004 [[hep-ph/0504050](#)]. [Erratum: *Phys.Rev.D* 72, 099902 (2005)].
- [96] S. Iguro and K. Tobe, “ $R(D^{(*)})$ in a general two Higgs doublet model,” *Nucl. Phys. B* **925** (2017) 560–606 [[arXiv:1708.06176](#)].
- [97] M. Aiko and S. Kanemura, “New scenario for aligned Higgs couplings originated from the twisted custodial symmetry at high energies,” *JHEP* **02** (2021) 046 [[arXiv:2009.04330](#)].
- [98] J. F. Gunion and H. E. Haber, “The CP conserving two Higgs doublet model: The Approach to the decoupling limit,” *Phys. Rev. D* **67** (2003) 075019 [[hep-ph/0207010](#)].
- [99] N. Craig, J. Galloway, and S. Thomas, “Searching for Signs of the Second Higgs Doublet.” [arXiv:1305.2424](#).
- [100] M. Carena, I. Low, N. R. Shah, and C. E. M. Wagner, “Impersonating the Standard Model Higgs Boson: Alignment without Decoupling,” *JHEP* **04** (2014) 015 [[arXiv:1310.2248](#)].
- [101] P. S. Bhupal Dev and A. Pilaftsis, “Maximally Symmetric Two Higgs Doublet Model with Natural Standard Model Alignment,” *JHEP* **12** (2014) 024 [[arXiv:1408.3405](#)]. [Erratum: *JHEP* 11, 147 (2015)].
- [102] M. E. Peskin and T. Takeuchi, “A New constraint on a strongly interacting Higgs sector,” *Phys. Rev. Lett.* **65** (1990) 964–967.
- [103] M. E. Peskin and T. Takeuchi, “Estimation of oblique electroweak corrections,” *Phys. Rev. D* **46** (1992) 381–409.

- [104] **Particle Data Group** Collaboration, “Review of Particle Physics,” *PTEP* **2022** (2022) 083C01.
- [105] J. M. Gerard and M. Herquet, “A Twisted custodial symmetry in the two-Higgs-doublet model,” *Phys. Rev. Lett.* **98** (2007) 251802 [[hep-ph/0703051](#)].
- [106] J. Alwall, *et al.*, “The automated computation of tree-level and next-to-leading order differential cross sections, and their matching to parton shower simulations,” *JHEP* **07** (2014) 079 [[arXiv:1405.0301](#)].
- [107] The numerical data of the production cross sections as well as the process and parameter cards for these analyses are available in <https://www.ttp.kit.edu/preprints/2022/ttp22-061/>.
- [108] F. Buccioni, *et al.*, “OpenLoops 2,” *Eur. Phys. J. C* **79** (2019) 866 [[arXiv:1907.13071](#)].
- [109] **ATLAS** Collaboration, “Measurement of the properties of Higgs boson production at $\sqrt{s} = 13$ TeV in the $H \rightarrow \gamma\gamma$ channel using 139 fb $^{-1}$ of pp collision data with the ATLAS experiment.” [arXiv:2207.00348](#).
- [110] S. Kanemura, T. Kubota, and E. Takasugi, “Lee-Quigg-Thacker bounds for Higgs boson masses in a two doublet model,” *Phys. Lett. B* **313** (1993) 155–160 [[hep-ph/9303263](#)].
- [111] A. G. Akeroyd, A. Arhrib, and E.-M. Naimi, “Note on tree level unitarity in the general two Higgs doublet model,” *Phys. Lett. B* **490** (2000) 119–124 [[hep-ph/0006035](#)].
- [112] A. Arhrib, “Unitarity constraints on scalar parameters of the standard and two Higgs doublets model,” in *Workshop on Noncommutative Geometry, Superstrings and Particle Physics*. 2000. [hep-ph/0012353](#).
- [113] A. Goudelis, B. Herrmann, and O. Stål, “Dark matter in the Inert Doublet Model after the discovery of a Higgs-like boson at the LHC,” *JHEP* **09** (2013) 106 [[arXiv:1303.3010](#)].
- [114] S. Iguro, S. Okawa, and Y. Omura, “Light lepton portal dark matter meets the LHC.” [arXiv:2208.05487](#).
- [115] M. Maniatis, A. von Manteuffel, O. Nachtmann, and F. Nagel, “Stability and symmetry breaking in the general two-Higgs-doublet model,” *Eur. Phys. J. C* **48** (2006) 805–823 [[hep-ph/0605184](#)].
- [116] P. M. Ferreira and D. R. T. Jones, “Bounds on scalar masses in two Higgs doublet models,” *JHEP* **08** (2009) 069 [[arXiv:0903.2856](#)].
- [117] N. G. Deshpande and E. Ma, “Pattern of Symmetry Breaking with Two Higgs Doublets,” *Phys. Rev. D* **18** (1978) 2574.
- [118] **ATLAS** Collaboration, “Search for charged Higgs bosons decaying into a top quark and a bottom quark at $\sqrt{s} = 13$ TeV with the ATLAS detector,” *JHEP* **06** (2021) 145 [[arXiv:2102.10076](#)].
- [119] **CMS** Collaboration, “Search for a charged Higgs boson decaying to charm and bottom quarks in proton-proton collisions at $\sqrt{s} = 8$ TeV,” *JHEP* **11** (2018) 115 [[arXiv:1808.06575](#)].
- [120] **ATLAS** Collaboration, “Search for a light charged Higgs boson in $t \rightarrow H^{+b}$ decays, with $H^{+} \rightarrow cb$, in the lepton+jets final state in proton-proton collisions at $\sqrt{s} = 13$ TeV with the ATLAS detector.”. <https://cds.cern.ch/record/2779169>.
- [121] **ATLAS** Collaboration, “Search for charged Higgs bosons decaying via $H^{\pm} \rightarrow \tau^{\pm}\nu_{\tau}$ in the τ +jets and τ +lepton final states with 36 fb $^{-1}$ of pp collision data recorded at $\sqrt{s} = 13$ TeV with the ATLAS experiment,” *JHEP* **09** (2018) 139 [[arXiv:1807.07915](#)].

- [122] **CMS** Collaboration, “Search for a light charged Higgs boson in the $H^\pm \rightarrow cs$ channel in proton-proton collisions at $\sqrt{s} = 13$ TeV,” *Phys. Rev. D* **102** (2020) 072001 [[arXiv:2005.08900](#)].
- [123] **CMS** Collaboration, “Search for resonant $t\bar{t}$ production in proton-proton collisions at $\sqrt{s} = 13$ TeV,” *JHEP* **04** (2019) 031 [[arXiv:1810.05905](#)].
- [124] S. Iguro and Y. Omura, “Status of the semileptonic B decays and muon g-2 in general 2HDMs with right-handed neutrinos,” *JHEP* **05** (2018) 173 [[arXiv:1802.01732](#)].
- [125] L. Di Luzio, M. Kirk, A. Lenz, and T. Rauh, “ ΔM_s theory precision confronts flavour anomalies,” *JHEP* **12** (2019) 009 [[arXiv:1909.11087](#)].
- [126] S. Iguro and Y. Omura, “The direct CP violation in a general two Higgs doublet model,” *JHEP* **08** (2019) 098 [[arXiv:1905.11778](#)].
- [127] **ATLAS** Collaboration, “Search for invisible Higgs boson decays with vector boson fusion signatures with the ATLAS detector using an integrated luminosity of 139 fb $^{-1}$.” <https://cds.cern.ch/record/2715447>.
- [128] **CMS** Collaboration, “Search for invisible decays of the Higgs boson produced via vector boson fusion in proton-proton collisions at $\sqrt{s} = 13$ TeV,” *Phys. Rev. D* **105** (2022) 092007 [[arXiv:2201.11585](#)].
- [129] **CMS** Collaboration, “Searches for additional Higgs bosons and vector leptoquarks in $\tau\tau$ final states in proton-proton collisions at $\sqrt{s} = 13$ TeV.” <http://cds.cern.ch/record/2803739>.
- [130] **CMS** Collaboration, “Search for nonresonant Higgs boson pair production in final state with two bottom quarks and two tau leptons in proton-proton collisions at $\sqrt{s} = 13$ TeV.” [arXiv:2206.09401](#).
- [131] F. A. Dreyer and A. Karlberg, “Vector-Boson Fusion Higgs Pair Production at N 3 LO,” *Phys. Rev. D* **98** (2018) 114016 [[arXiv:1811.07906](#)].
- [132] **ATLAS** Collaboration, “Search for a heavy Higgs boson decaying into a Z boson and another heavy Higgs boson in the $\ell\ell b\bar{b}$ final state in pp collisions at $\sqrt{s} = 13$ TeV with the ATLAS detector,” *Phys. Lett. B* **783** (2018) 392–414 [[arXiv:1804.01126](#)].
- [133] **CMS** Collaboration, “Search for new neutral Higgs bosons through the $H \rightarrow ZA \rightarrow \ell^+ \ell^- b\bar{b}$ process in pp collisions at $\sqrt{s} = 13$ TeV,” *JHEP* **03** (2020) 055 [[arXiv:1911.03781](#)].
- [134] R. V. Harlander, S. Liebler, and H. Mantler, “SusHi: A program for the calculation of Higgs production in gluon fusion and bottom-quark annihilation in the Standard Model and the MSSM,” *Comput. Phys. Commun.* **184** (2013) 1605–1617 [[arXiv:1212.3249](#)].
- [135] R. V. Harlander, S. Liebler, and H. Mantler, “SusHi Bento: Beyond NNLO and the heavy-top limit,” *Comput. Phys. Commun.* **212** (2017) 239–257 [[arXiv:1605.03190](#)].
- [136] X.-Q. Li, J. Lu, and A. Pich, “ $B_{s,d}^0 \rightarrow \ell^+ \ell^-$ Decays in the Aligned Two-Higgs-Doublet Model,” *JHEP* **06** (2014) 022 [[arXiv:1404.5865](#)].